Itinerant-electron-type helical–spin-glass reentrant transition in $Cr_{0.81}Mn_{0.19}Ge$

T. Sato
Department of Instrumentation Engineering, Faculty of Science and Technology, Keio University, 3-14-1 Hiyoshi, Kohoku-ku, Yokohama-shi, Kanagawa, Japan

T. Ando and T. Oku
Department of Materials Science, Faculty of Science and Technology, Keio University, 3-14-1 Hiyoshi, Kohoku-ku, Yokohama-shi, Kanagawa, Japan

M. Furusaka
National Laboratory for High Energy Physics, 1-1 Oho, Tsukuba-shi, Ibaraki, Japan
(Received 21 October 1993; revised manuscript received 24 January 1994)

Small-angle neutron-scattering and some magnetic measurements of $Cr_{0.81}Mn_{0.19}Ge$ gave evidence of a double transition, from a paramagnetic to a helical magnetic state, and to a mixed state of helical and spin-glass-like ordering with decreasing temperature. The helical spin modulation, having a long period (from 360 Å at 5.3 K to 420 Å at 12.5 K), indicates the nature of an itinerant-electron-type magnet, and the reentrant transition is interpreted on the basis of the interacting spin fluctuation.

I. INTRODUCTION

Spin-glass problems have rarely been discussed in itinerant-electron description. The early idea of the Stoner glass[1] predicted the possible spin-glass transition through the interaction between weakly localized spins, and was applied to some impurity systems with a high Kondo temperature. However, such a viewpoint has not been followed up to the point where its validity can be experimentally determined. The reentrant transition, the most attractive theme regarding frustrated spin systems in the past decade, has scarcely been explained in such a manner. Provided the reentrant nature was reconsidered from the viewpoint mentioned above, there would be some criteria for evaluating the itinerant picture of spin glass. This is because the itineracy in the spin freezing state can be well characterized in connection with the well-characterized magnetism of the ordered state. To obtain some evidence for such a reentrant transition, due to the local spin fluctuations, we have paid attention to some impurity systems with an exchange-enhanced magnetic matrix. This paper presents experimental evidence supporting the itinerant-electron-type reentrant transition in $Cr_{0.81}Mn_{0.19}Ge$.

Chromium monogermanide (CrGe) with the cubic $B20$ structure shows a nearly ferromagnetic nature.[2] The solid solution $Cr_{1-x}Mn_xGe$ with $0.09 \leq x \leq 0.15$ has weak ferromagnetic nature, and the large content of Mn ($x \geq 0.24$) leads to frustrated spins.[3,4] In the intermediate Mn concentration region ($0.17 \leq x \leq 0.21$), we found some characteristics expected of a reentrant spin glass, i.e., the rapid increase in magnetization at T_c and some irreversible behavior at temperatures below T_{sh} [lower than T_c (Refs. 3,5)]. On the other hand, the spontaneous magnetic moment of $Cr_{0.81}Mn_{0.19}Ge$, obtained from the $H=0$ extrapolation of a high-field ($H > 400$ Oe) magnetization curve,[5] is about $0.9\mu_B$/Mn atom at 4.3 K, which is much smaller than the effective magnetic moment of $3.6\mu_B$/Mn atom determined in the paramagnetic region.[3] This suggests an itinerant-electron nature in the ordered state of $Cr_{0.81}Mn_{0.19}Ge$. The field-dependent magnetization obtained below 400 Oe, however, suggested no spontaneous magnetization.

In the present work, we performed the ac and dc magnetic measurements and the small-angle neutron-scattering (SANS) measurements of $Cr_{0.81}Mn_{0.19}Ge$. We clarify the magnetic nature in the ordered states, and show that the characteristic irreversibility at low temperature is interpreted in terms of the itinerant-electron-type helical–spin-glass reentrant transition.

II. EXPERIMENTAL PROCEDURE

The polycrystalline $Cr_{0.81}Mn_{0.19}Ge$ sample was prepared, as shown in the previous paper.[3] The sample for magnetic measurements was shaped to a sphere 3 mm in diameter, and a plate sample 1 mm thick was used for the neutron-scattering measurements. The ac susceptibility measurement was performed using the Hartshorn-type bridge.[4] We obtained the linear and nonlinear terms from the ac susceptibility data. The low-field dc susceptibility and the thermoremanent magnetization (TRM) were measured using a Quantum Design MPMS2 superconducting quantum interference device (SQUID) magnetometer. The TRM data were analyzed on the basis of the stretched exponential and the power-law-type relaxation functions. The SANS measurements were performed using a small-angle neutron-scattering (SAN) spectrometer, installed at the pulsed neutron facility at the National Laboratory for High Energy Physics (KEK). The magnetic contribution was separated using the scattering intensity obtained at 50 K where the spins are completely disordered. We also measured the neutron-scattering intensity in magnetic field which was applied along a direction perpendicular to the incident direction of neutrons.

III. EXPERIMENTAL DATA AND ANALYSIS

A. Magnetic data

Figure 1 shows some temperature-dependent ac and dc magnetic susceptibilities of $Cr_{0.81}Mn_{0.19}Ge$. The real part of linear ac susceptibility χ_{ac} ($f=105$ Hz and $h=6$ Oe) shows a maximum at $T_c=13.0$ K. On the other hand, in the imaginary part, the two maxima with negative sign are observed at 9.5 and ~ 13 K, which suggest the double transition. The nonlinear susceptibility $\frac{3}{4}\chi_2' h_0^2$, which is defined as the response at the third harmonic,[6] shows a maximum at $T_f=10.6$ K and diverges with a negative sign at a temperature just below 13 K. Such behavior in the nonlinear susceptibility has been discussed in connection with the phase transition temperatures in the reentrant spin glass $(Pd_{0.9966}Fe_{0.0034})_{0.95}Mn_{0.05}$.[7] Here, we note that T_f in the nonlinear susceptibility is sensitive to the frequency and magnetic field.

The dc susceptibility χ_{dc} measured at 0.5 Oe shows a maximum at 12.9 K, below which the irreversible behavior is observed according to the sample cooling procedure. The zero-field-cooled (ZFC) susceptibility, furthermore, has a hump around 8.5 K, although the field-cooled (FC) data do not show any anomalous behavior at the hump temperature. Such a hump in low-field dc susceptibility was regarded as a sign of a reentrant transition in the reentrant NiMn alloy,[8] in which the irreversible behavior was also observed up to a temperature significantly higher than the hump temperature.

The TRM data in Fig. 2(a) show the long-time relaxation behavior at temperatures below ~ 10 K as expected for a spin freezing state, where the samples were cooled in $H_c=100$ Oe from 50 K and the waiting time was about 50 sec. Figure 2(b) shows the decrement S of the logarithmic time-dependent magnetization:

$$M=M_0+S\log_{10}t \ . \tag{1}$$

The largest value of S is observed between 4 and 5 K. Such a maximum in the decrement has been explained as a characteristic relevant to the spin freezing temperature.[9] Furthermore, we analyzed the TRM data on the basis of the common relaxation functions, namely, the superposition of a constant term and a stretched exponential:

$$M=M_0'+M_1\exp[-(t/\tau)^{1-n}] \ , \tag{2}$$

and the superposition of a power-law and a constant term:

$$M=M_0''+\sigma_0 t^{-m} \ . \tag{3}$$

The TRM data at temperatures below 4 K are well described by Eq. (2), as shown in Figs. 3(a)–3(c) which show the linear relation between $\log_{10}[-(d/dt)\ln_{10}(M-M_0')]$ and $\log_{10}t$. As abridged in Table I, the best-fitted parameters n and τ increase and decrease with increasing temperature, respectively. On the other hand, the extraordinarily small value of τ ($\sim 10^{-14}$ sec) at 5 K suggests that Eq. (2) is insufficient relaxation function for the TRM data of $Cr_{0.81}Mn_{0.19}Ge$ above 5 K. The higher temperature relaxation is well described by Eq. (3), as shown in Figs. 3(d)–3(f) in which the double logarithmic plots of

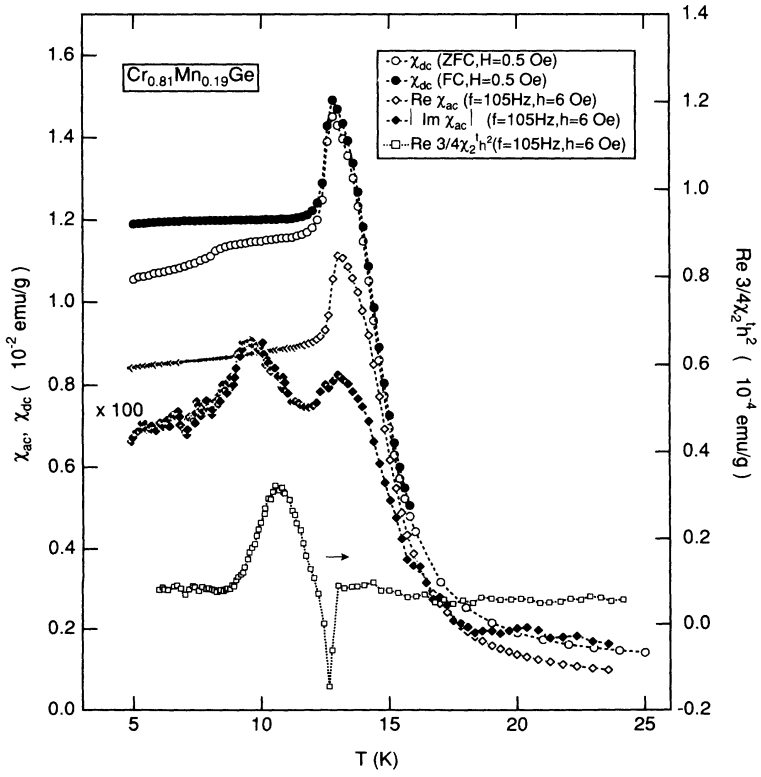

FIG. 1. Temperature-dependent ac and dc susceptibilities of $Cr_{0.81}Mn_{0.19}Ge$. The real and imaginary parts of linear ac susceptibility χ_{ac} and the nonlinear susceptibility $\frac{3}{4}\chi_2' h_0^2$ are measured at $f=105$ Hz and $h=6$ Oe. The dc susceptibility χ_{dc} is measured at $H=0.5$ Oe under zero field cooling (ZFC) and field cooling (FC) conditions.

$-dM/dt$ as a function of t yield straight line behavior. The best-fitted exponent m in Eq. (3) increases with increasing temperature (Table I). Such change in the relaxation function and the rapid decrease in τ are suggestive of the spin freezing around 5 K. The same feature of the relaxation of the thermoremanent magnetization has been observed in the other reentrant spin-glass systems [NiMn (Ref. 8) and AuFe (Ref. 10)].

These magnetic data obviously indicate the spin-glass-like ordering, appearing below the high-temperature ordered state of $T_c = 13$ K. However, the evaluation of the spin freezing temperature significantly depends on the experimental techniques which reflect different time scales peculiar to them, i.e., 10.6 K (ac susceptibility), 8.5 K (dc susceptibility), and ~5 K (TRM).

B. SANS data

Figure 4 shows the SANS intensity of $Cr_{0.81}Mn_{0.19}Ge$ in zero field as a function of the momentum transfer q. An intensity peak at q_0 was found at temperatures below 14 K, which indicates a modulated spin structure in the zero field magnetic state. Figure 5(a) shows the temperature dependence of the scattering intensities at $q = 0.012$, 0.014, 0.016, 0.018, and 0.020 Å^{-1}, and the integrated intensity from 0.01 to 0.04 Å^{-1}. The maximum observed in the temperature-dependent integrated intensity around 7 K suggests that the modulated spin state becomes unstable at low temperatures. The q-dependent scattering intensity can be fitted with the following Lorentzian and constant term:

$$I(q) = I_c + \frac{I_0 \Delta q_{\text{tot}}^2}{(q - q_0)^2 + \Delta q_{\text{tot}}^2} . \quad (4)$$

Figure 5(b) shows the best-fitted peak position q_0 and linewidth Δq, where Δq was obtained from Δq_{tot} by evaluating the resolution inherent in the apparatus.[11] The period of the modulation, estimated as $2\pi/q_0$, decreases with decreasing temperature, i.e., 420 Å at 12.5 K to 360 Å at 5.3 K. On the other hand, the coherent length, estimated from Δq by assuming the one-dimensional modulated spin structure,[12] increases with decreasing temperature over the range from 2.5 to 5 periods of spin modulation. We should note that these values of q_0 and Δq scarcely show anomalous behavior around 7 K. Although we cannot explain a lack of anomalous behavior around 7 K with the present data, it may suggest that the instability of the modulated spin state is starting from a temperature higher than 7 K.

Furthermore, some additive information about the modulated spin structure can be obtained from the SANS measurements in magnetic fields. Figures 6(a) and 6(b) show the x and y components of the neutron-scattering intensity measured in magnetic fields up to 400 Oe, where the incident direction of neutrons was perpendicular to the xy plane and the magnetic field was applied parallel to the x direction.[13] The intensity in 100 Oe is essentially identical to that in 0 Oe. The x component shows the two intensive peaks at q_0' and q_0'' in 200 Oe, where the lower q_0' is identical to q_0 determined in zero field. Upon applying to a field of 400 Oe, these peaks became more intensive. Here, we can note the relation of $q_0'' \approx \sqrt{2} q_0'$. In the same field range, the peak intensity of the y component rapidly decreases, while the scattering in the lower q region notably intensifies. Thus the field-dependent SANS data are interpreted by assuming that the spin structure in zero field is a helical one as follows.

(1) Below 100 Oe, the spins of the helical structure are restricted in the planes perpendicular to the specified crystal axis, which would be identified with the ⟨100⟩ direction as mentioned below. Therefore, the scattering is isotropic in the present polycrystalline sample.

(2) In a field from 200 to 400 Oe, the helical spin structure changes to a conical type one whose screw axis preferentially turns parallel to the direction of the applied field. Such a picture is supported by a notably intensified peak at q_0' in the x component, and by an appearance of a very low q scattering in the y component. This is because the former reflects an increase in scattering from the spin components in the plane perpendicular to the field direction, and the latter indicates the scattering from long-range ferromagnetic spins along the x direction. The additive scattering at q_0'' in the x component suggests the appearance of a higher harmonic, originating from the interaction of helical structures with different wave vec-

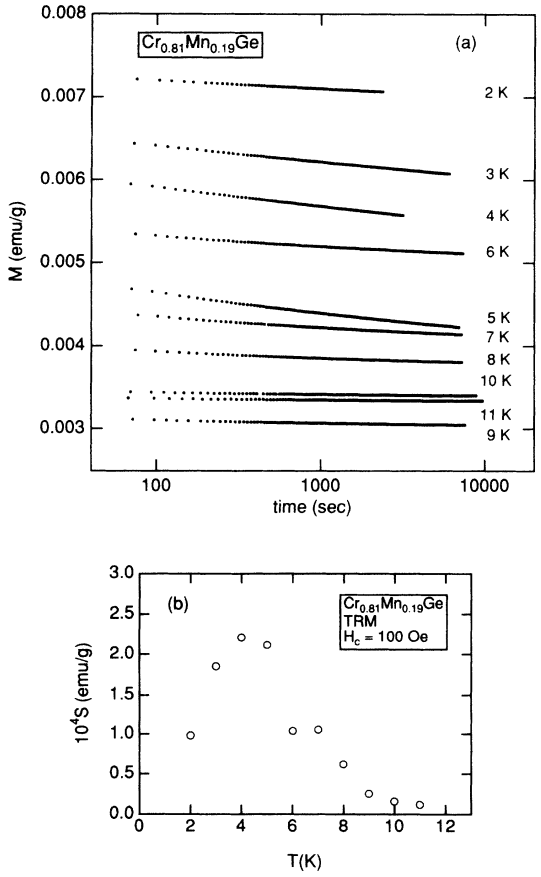

FIG. 2. (a) Time dependence of the thermoremanent magnetization (TRM) of $Cr_{0.81}Mn_{0.19}Ge$ measured after sample was cooled in $H = 100$ Oe from 50 K. (b) The decrement S of logarithmic time-dependent magnetization is plotted as a function of temperature.

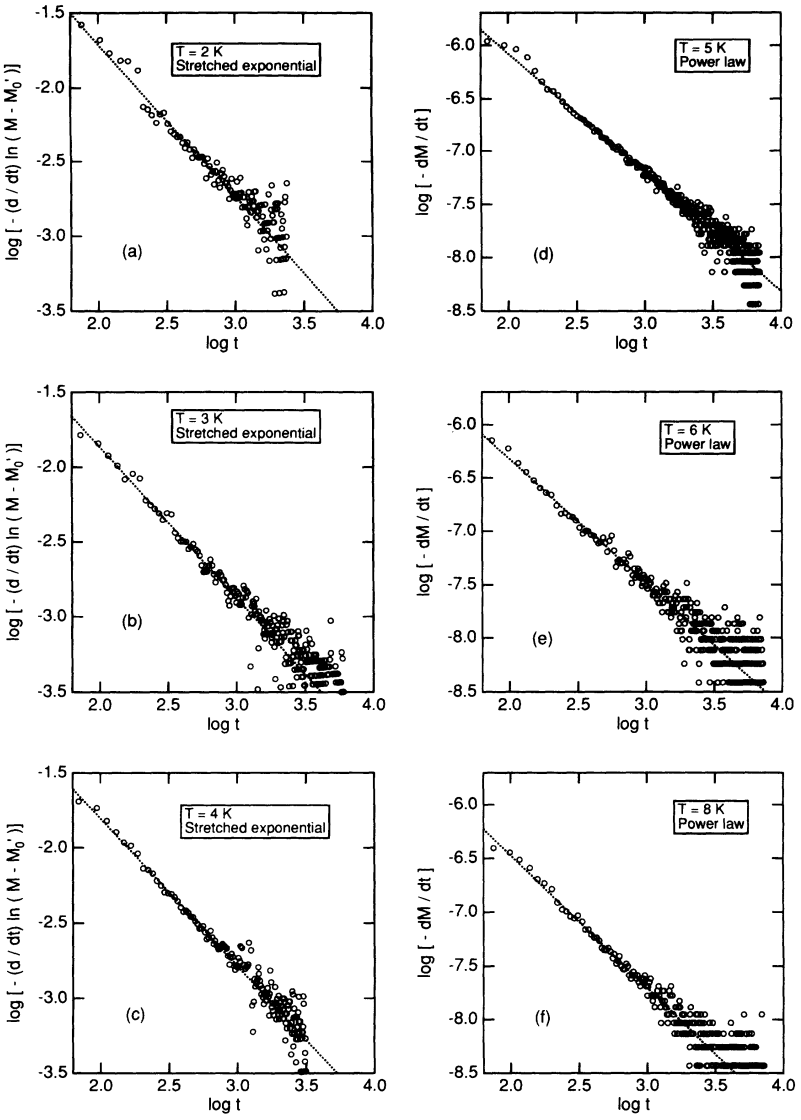

FIG. 3. Double logarithmic plot (base 10) of $-(d/dt)\ln(M-M_0')$ as a function of t at 2 K (a), 3 K (b), and 4 K (c). Double logarithmic plot (base 10) of $-dM/dt$ as a function of t at 5 K (d), 6 K (e), and 8 K (f).

TABLE I. Parameters from power-law and stretched exponential fits for TRM data of $Cr_{0.81}Mn_{0.19}Ge$.

	Power law			Stretched exponential			
T (K)	M_0'' (emu/g)	σ_0 (emu/g)	m	M_0' (emu/g)	M_1 (emu/g)	τ (sec)	n
2				$(6.7\pm0.1)\times10^{-3}$	$(1.8\pm0.2)\times10^{-3}$	1.5±0.6	0.93±0.01
3				$(5.0\pm0.3)\times10^{-3}$	$(6.3\pm1.0)\times10^{-3}$	$(5.5\pm4.5)\times10^{-3}$	0.96±0.01
4				$(4.6\pm0.3)\times10^{-3}$	$(1.0\pm0.1)\times10^{-2}$	$(1.1\pm1.0)\times10^{-6}$	0.96±0.01
5	$(3.7\pm0.1)\times10^{-3}$	$(1.8\pm0.1)\times10^{-3}$	0.13±0.01	$(3.8\pm0.3)\times10^{-3}$	$(3.8\pm0.4)\times10^{-2}$	$\sim10^{-14}$ [a]	0.96±0.01
6	$(4.9\pm0.1)\times10^{-3}$	$(8.9\pm0.1)\times10^{-4}$	0.16±0.02				
7	$(3.9\pm0.1)\times10^{-3}$	$(9.3\pm0.3)\times10^{-4}$	0.19±0.02				
8	$(3.7\pm0.1)\times10^{-3}$	$(6.1\pm0.4)\times10^{-4}$	0.23±0.02				
9	$(3.0\pm0.1)\times10^{-3}$	$(3.3\pm0.5)\times10^{-4}$	0.31±0.04				
10	$(3.4\pm0.1)\times10^{-3}$	$(1.8\pm0.4)\times10^{-4}$	0.27±0.05				
11	$(3.3\pm0.1)\times10^{-3}$	$(1.4\pm0.3)\times10^{-4}$	0.27±0.05				

[a]The order of this value can be estimated.

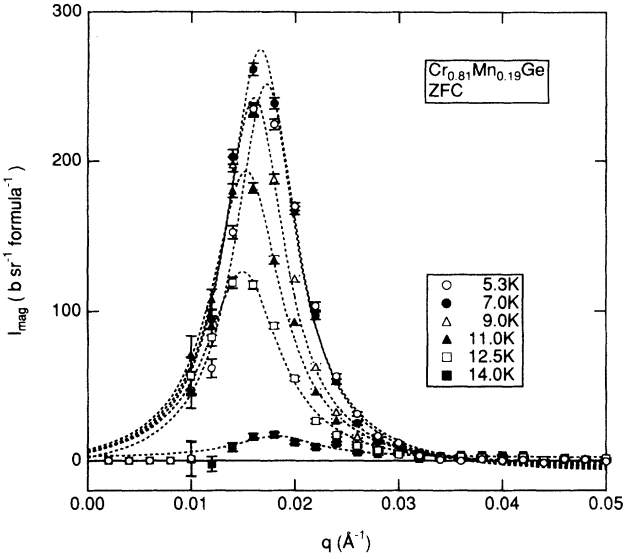

FIG. 4. Magnetic contribution in small-angle neutron-scattering intensity of $Cr_{0.81}Mn_{0.19}Ge$ in zero field is plotted as a function of momentum transfer q, in which the data are analyzed using Eq. (4).

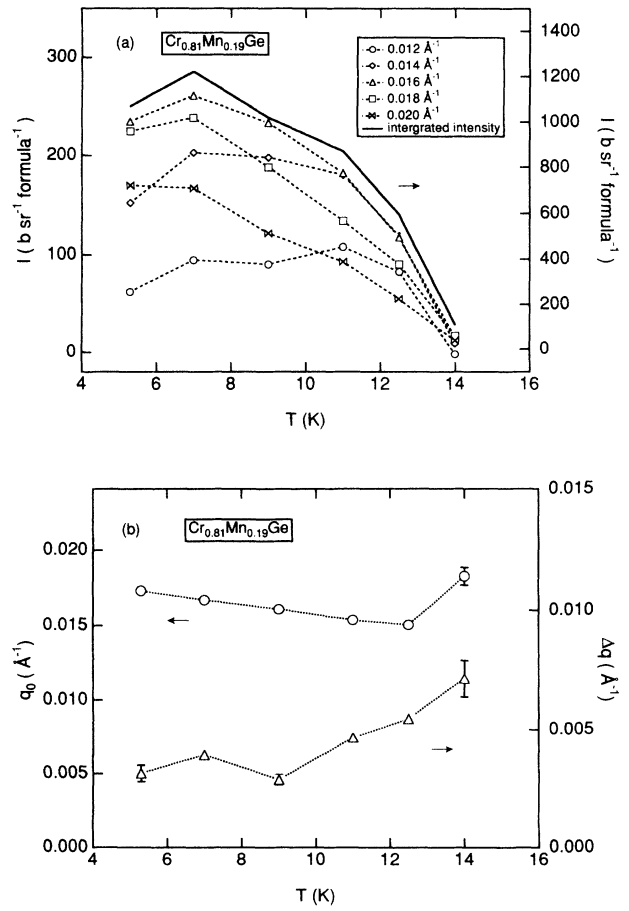

FIG. 5. (a) The scattering intensity of $Cr_{0.81}Mn_{0.19}Ge$ at $q=0.012$, 0.014, 0.016, 0.018, and 0.020 Å^{-1}, and the integrated intensity within the q range from 0.01 to 0.04 Å^{-1}. (b) The temperature dependence of the best-fitted peak position q_0 and linewidth Δq.

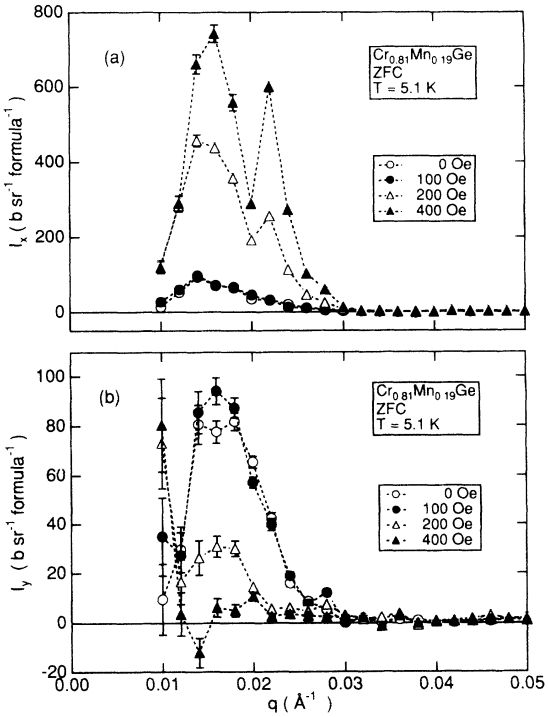

FIG. 6. The x (a) and y components (b) of the neutron-scattering intensity of $Cr_{0.81}Mn_{0.19}Ge$ measured at 5.1 K in fields up to 400 Oe under zero field cooling conditions.

tors, as was reported for the itinerant-type helimagnet MnSi.[14] Therefore, we can estimate that the wave vector of the helical spins is along the ⟨100⟩ direction based on the relation $q_0'' = \sqrt{2} q_0'$.

Such a field-dependent spin arrangement is consistent with the peculiar behavior of the magnetization process previously reported.[5] Therefore, we can claim that $Cr_{0.81}Mn_{0.19}Ge$ has a helical spin structure with a long period at temperatures below ~13 K, which would be characterized as an itinerant-electron-type one. Furthermore, the helical spin arrangement would become unstable at low temperatures as suggested by the decrease in scattering intensity at lower temperatures. This would support the freezing of spins at low temperatures as suggested from the magnetic data. We cannot detect any scattering relevant to the spin freezing in the present q range, however, in contrast to the scattering around $q=0$ observed in the other reentrant materials.[15,16] This characteristic may be attributed to a very long spin correlation in the spin freezing state, so that the scattering no longer contributes in the present q range.

IV. DISCUSSION FOR MAGNETIC NATURE OF $Cr_{0.81}Mn_{0.19}Ge$

Both the present magnetic and SANS data support the reentrant spin-glass transition in $Cr_{0.81}Mn_{0.19}Ge$, in which the spin-glass-like characteristics coexist with the itinerant-electron-type helical spin structure. Although detailed spin configuration in the reentrant state cannot be depicted at this point in time, we may predict the possible interdomain freezing, where the domain size may be

characterized by the coherent length of helical spin ordering. Theoretical background of the itinerant-type helical spin structure was proposed in terms of the self-consistent renormalization theory,[17] which gave a qualitative explanation for a stable helical spin arrangement in zero field and the helical-conical change with an applying field. For the helical spin arrangement, with a long period in a crystal structure lacking inversion symmetry, e.g., $B20$ type MnSi and $Cr_{1-x}Mn_xGe$, the important role of the spin-orbit interaction has been indicated.[18,19] This suggested that helical spins are stabilized by the Dzyaloshinsky-Moriya-type spin interaction, which corresponds to the second order on free energy expanded in powers of spin density. On the other hand, spin-glass-like ordering should originate from higher-order spin interaction. When the magnitude of the spin increases with decreasing temperature, the spin-glass-like ordering would become more stable compared to the helical spin structure. Thus, we can qualitatively interpret the helical–spin-glass reentrant transition from the itinerant-electron viewpoint. Finally, we would note that the amorphous $Cr_{1-x}Mn_xGe$ system shows only pure spin glass, with a transition temperature which decreases with decreasing Mn concentration and reaches 0 K at zero Mn content.[20] Such a magnetic phase diagram is in contrast to that of the crystalline system, in which the transition temperature must reach 0 K at a finite Mn content.[3] This difference reflects the itinerant-electron nature in the spin-glass-like state of crystalline $Cr_{0.81}Mn_{0.19}Ge$,[1] since the amorphization process should result in more-developed localization of Mn spins.

$Cr_{0.81}Mn_{0.19}Ge$ shows a double transition from a paramagnetic to a helical magnetic state at $T \sim 13$ K, and to a mixed phase of helical and spin-glass-like ordering with decreasing temperature. Both in the helimagnetic state and the mixed state, the magnetic nature is interpreted in terms of the itinerant-electron picture. We conclude that the present reentrant transition is characterized in terms of an interacting spin fluctuation.

ACKNOWLEDGMENTS

This work was partially supported under a Grant-in-Aid for Science Research from the Ministry of Education, Science and Culture, by Asahi Glass Foundation, and by Kanagawa Academy of Science and Technology Foundation.

[1]J. A. Hertz, Phys. Rev. B **19**, 4796 (1979).
[2]T. Sato and M. Sakata, J. Phys. Soc. Jpn. **52**, 1807 (1983).
[3]T. Sato, J. Kozu, K. Oshiden, T. Nemoto, E. Ohta, M. Sakata, T. Goto, and T. Sakakibara, J. Phys. Soc. Jpn. **57**, 639 (1988).
[4]T. Nemoto, T. Sato, E. Ohta, and M. Sakata, J. Magn. Magn. Mater. **78**, 43 (1989).
[5]T. Sato, T. Nemoto, E. Ohta, M. Sakata, T. Sakakibara, and T. Goto, J. Magn. Magn. Mater. **70**, 411 (1987).
[6]S. Chikazawa, Y. G. Yuochunas, and Y. Miyako, J. Phys. Soc. Jpn. **49**, 1276 (1980).
[7]T. Sato and Y. Miyako, J. Phys. Soc. Jpn. **51**, 1394 (1981).
[8]R. M. Roshko and W. Ruan, J. Phys. I **1**, 1809 (1991); J. Phys. Condens. Matter **4**, 6451 (1992).
[9]C. N. Guy, J. Phys. F **8**, 1309 (1978).
[10]P. Mitchler, R. M. Roshko, and W. Ruan, J. Phys. I **2**, 2299 (1992).
[11]Y. Ishikawa, M. Furusaka, N. Niimura, M. Arai, and K. Hasegawa, J. Appl. Cryst. **19**, 229 (1986).
[12]David W. L. Hukins, *X-ray Diffraction by Disordered and Ordered Systems* (Pergamon, New York, 1981), Chaps. VIII and IX.
[13]T. Sato, T. Ando, T. Watanabe, S. Itoh, Y. Endoh, and M. Furusaka, Phys. Rev. B **48**, 6074 (1993).
[14]Y. Ishikawa, K. Tajima, D. Bloch, and M. Roth, Solid State Commun. **19**, 525 (1976).
[15]G. Aeppli, S. M. Shapiro, R. J. Birgeneau, and H. S. Chen, Phys. Rev. B **28**, 5160 (1983).
[16]K. Motoya, S. M. Shapiro, and Y. Muraoka, Phys. Rev. B **28**, 6183 (1983).
[17]T. Moriya, Solid State Commun. **20**, 291 (1976).
[18]O. Nakanishi, A. Yanase, A. Hasegawa, and M. Kataoka, Solid State Commun. **35**, 995 (1980).
[19]P. Beck and M. H. Jensen, J. Phys. C **13**, L881 (1980).
[20]T. Sato, M. Kamei, T. Nemoto, E. Ohta, M. Sakata, T. Goto, and T. Sakakibara, J. Phys. F. **18**, 1593 (1988).